Dry Wear and Friction Properties of an A356/SiC Foam Interpenetrating Phase Composite

D. Cree and M. Pugh*
Department of Mechanical Engineering, Concordia University
1455 de Maisonneuve Blvd. West
Montreal, Canada H3G 1M8
pugh@encs.concordia.ca
*Corresponding author. 1-514-848-2424 ext. 4190, Fax. 1-514-848-3175, e-mail: pugh@encs.concordia.ca

ABSTRACT

The dry sliding wear and friction behaviors of A356 aluminum alloy and a hybrid composite of A356 aluminum alloy and silicon carbide foam in the form of an interpenetrating phase composite were evaluated using a ball-on-disk apparatus at ambient conditions. The stationary 6.35 mm alumina ball produced a wear track (scar) diameter of 7 mm on the rotating specimen surface. Three different loads; 5 N, 10 N and 20 N were applied at a constant sliding speed of 33 mm/s for both materials. Wear tracks were characterized with a scanning electron microscope and measured with an optical surface profilometer. In general, this novel A356/SiC foam composite reduced the friction coefficient and wear rate from that of the base alloy for all loading conditions. In addition, as the load increased, the friction coefficient and wear rate decreased for both materials. The results indicate the composite could be used in light-weight applications where moderate strength and wear properties are needed.

Keywords: A356; silicon carbide foam; interpenetrating composite; hybrid; tribological behavior

1. Introduction

Metal-ceramic hybrid composites containing aluminum/SiC/carbon have been shown to have improved wear properties over their monolithic alloys [1]. Conventional ceramic reinforcements are in the form of discontinuous particles, whiskers and continuous/short fibres. Interpenetrating phase composites (IPCs) are less common but are gaining much attention due to their three-dimensional network structure having two, distinct, interconnected phases; a ceramic phase and a metallic phase. This unique arrangement of matrix and reinforcement provides high strength-to-weight and stiffness-to-weight ratios which are ideal for use in lightweight applications. In an earlier work, this Al/SiC foam three-dimensional infiltrated composite structure was shown to have intermediate mechanical and thermal properties [2]. For example, Raj et al. [3] found the toughness of ceramics can be increased by the addition of a ductile metal. They also established that a higher toughness is possessed by a composite where both the metal and ceramic phases form a continuous network as opposed to having the same volume fraction of discrete, isolated metal particles distributed in the composite. The current study provides a new insight into the wear and friction properties of an A356 aluminum alloy/silicon carbide (SiC) foam composite.

Wear properties of aluminum alloys can be improved by the addition of a second ceramic phase provided there is good interface bonding between the ceramic and metal phases [4]. Similar to discontinuous reinforcements, continuous ceramic reinforcing structures have shown to have lower wear rates than the base metal alloy, in addition to a lower density than conventional ceramic particulate metal matrix composites (MMC's) due to a lower reinforcement volume fraction [5]. In addition to incorporating a ceramic phase to improve the wear, friction and seizure properties of aluminum, external lubrication between mating parts or infused lubrication into a porous material can be in the form of oil or grease, water or graphite

particles embedded into the composite. However, oil run-off can contaminate the environment; water can lead to corrosion of components while the addition of graphite in the form of particles or fibers is attractive for dry or self-lubricating materials. Such materials do not require lubricant replenishment at regular intervals since the lubricating material forms an internal component of the composite. As the composite slides/rubs against a mating surface, the solid carbon/graphite lubricant is depleted and in so doing, transfers to form a protective lubricating film. Self-lubricating materials are ideal for reducing maintenance and for use in wear locations where access is restricted. For instance, aluminum alloys with graphite particulates have recently been investigated for their tribological properties [6]. Interestingly the struts of the SiC ceramic foam utilized in this research have a carbon interior surrounded by a SiC shell. This unique structure may provide a dual purpose; self-lubricating mechanism and improved wear and friction properties.

The majority of wear studies on light-metal infiltrated, three-dimensional, network structures focus on alumina (Al_2O_3)/aluminum alloy IPCs. In contrast, this work investigates the dry abrasive wear and friction properties of an alumina ball sliding against A356 aluminum alloy and A356/SiC foam composite with 12% volume fraction of SiC network reinforcement.

2. Experimental Procedure

2.1 Materials

The matrix employed in this study is an A356 aluminum casting alloy supplied by Alcan Inc. with the following chemical composition; 92.3Al, 7.1Si**,** 0.38Mg, 0.13Ti and 0.1Fe (wt%). The reinforcement is commercially available Ultrafoam^{TM} 100 pores per linear inch (PPI) SiC ceramic foam (Ultramet). The SiC foam is reported to have a relative density of 12% with a bulk density and theoretical density of 0.37 gcm^{-3} and 3.2 gcm^{-3}, respectively. The approximate cell

diameter and window diameter are 480 μm and 150 μm, respectively. The morphology of the as-received SiC ceramic foam and the strut triangular geometry is shown in Figure 1. As shown in Figure 2 the struts of the Ultramet SiC foam are not pure SiC but have a carbon interior. Moreover, the SiC struts are not monolithic but form a multi-layered structure with each SiC layer separated by a carbon interface. After employing an oxidation treatment to the as-received SiC foam and given the density and mass of each component a volume fraction of SiC and carbon of 0.77 and 0.23, respectively were obtained. The details for producing the A356/SiC foam composite employing a low vacuum infiltration manufacturing process has been reported elsewhere [2]. To study the aluminum alloy grain structure, the as-cast A356/SiC foam composite sample was first ground to 1200 grit, followed by polishing to 1 micron with mono-crystalline diamond suspension. The sample was then etched for 5 seconds in a mixture of 1 mL Hydrofluoric acid and 200 mL of distilled water. Images of the etched surface were obtained using SEM and EDS to determine the silicon areas. The wear tests were conducted on sample cross-sections measuring 10 x 10 x 25 mm.

2.2 Wear test

The dry wear and sliding friction behaviour was studied using a ball-on-disk tribometer type apparatus as shown in Figure 3. The test equipment consists of a stationary alumina ball, a variable load (dead weight) and a specimen attached to a rotating disc. For each test, a new 6.35 mm diameter alumina ball (Hv=1700 kg/mm^2, surface finish: Ra = 3μm) Grade C25 (polished) was used (Hoover Precision Products). All samples were tested for 30 minutes at three normal loads of 5 N, 10 N and 20 N and a constant sliding speed of 33 mm/s at ambient temperature. The sliding distance (S) for the 30 minute test based on the wear track radius (3.5 mm), and disk rotational speed of 100 rpm was 66 m.

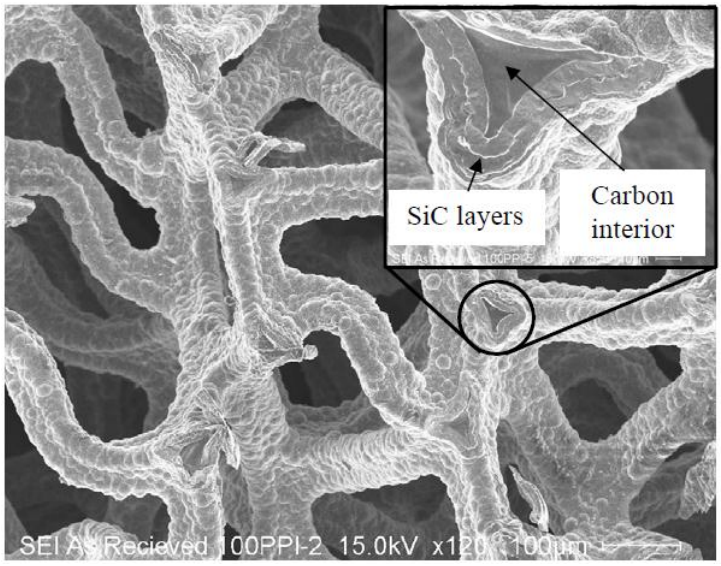

Figure 1. Morphology of the as-received SiC ceramic foam.

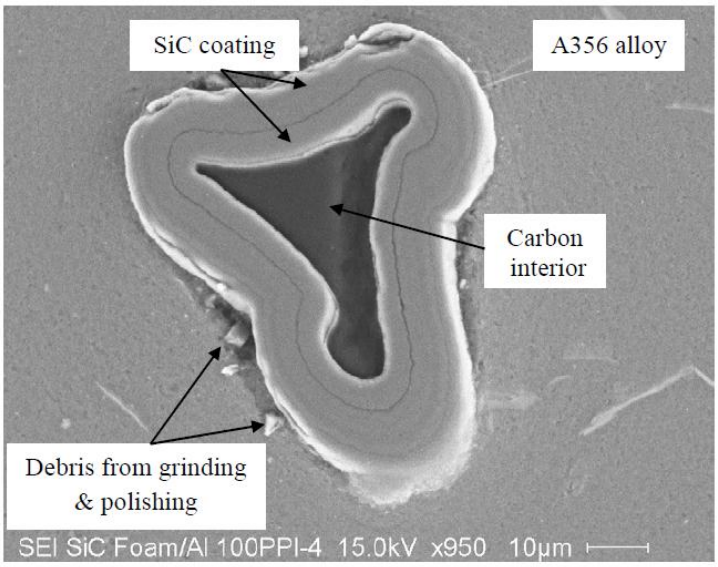

Figure 2. Typical triangular microstructural cross-section of the A356/SiC foam composite.

After the wear test, the total wear-track worn volume from the penetration of the alumina ball into the face of the composite was measured by multiplying the cross-sectional wear track area by the length of the wear track. The wear track cross-sectional area profile was measured using an optical surface profilometer (Dektak 3030ST) at four different places and averaged. The wear rate (K) was evaluated using Equation 1, where V_w is the total wear track worn volume and

S is the sliding distance. For all experiments, the coefficient of friction was established at a sliding distance of 66 m.

$$K=V_w / S \quad (1)$$

Both the unreinforced A356 aluminum alloy and the A356/SiC foam composite structure were examined prior to and after testing by a scanning electron microscope (SEM), JOEL 840A, with an acceleration voltage of 10-15 kV.

The hardness of the A356 unreinforced aluminum alloy, the A356/SiC foam composite and the wear track area of both materials were measured using a Vickers macrohardness tester under a 5 kg load. Five indentations of each sample were performed and averaged.

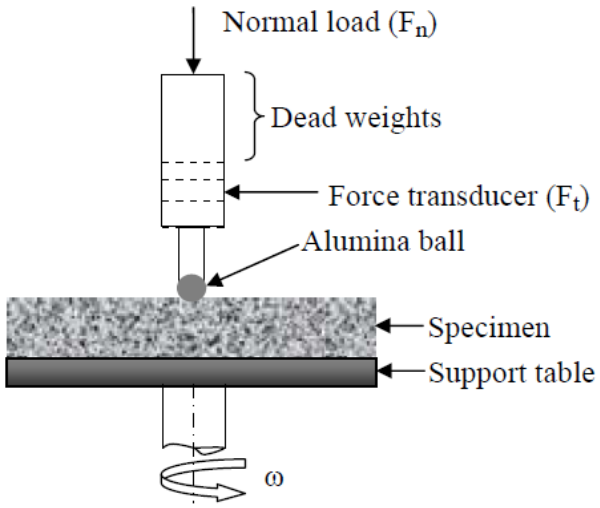

Figure 3. Schematic diagram of ball-on-disc tribometer apparatus.

3. Results and Discussion

3.1 Microstructure

The microstructure of the as-cast A356/SiC alloy composite is shown in Figure 4 and Figure 5. Both phases are continuous throughout the composite. Prior to etching, as shown in the polished sample of the optical micrograph (100x), Figure 4, upon slow cooling, the aluminum grains have

grown in the form of dendrite structures. Between the SiC struts, the grains have formed long and narrow outlines. Subsequent to etching, Figure 5 shows the dispersed silicon between the aluminum dendrite structures and is depicted by a coarse acicular morphology.

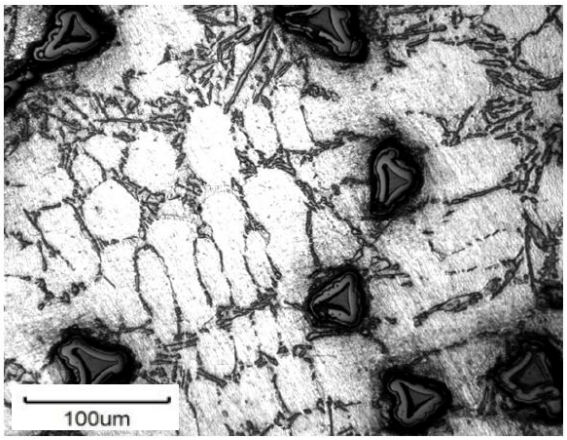

Figure 4. As-cast optical microstructure of the A356/SiC foam composite prior to etching.

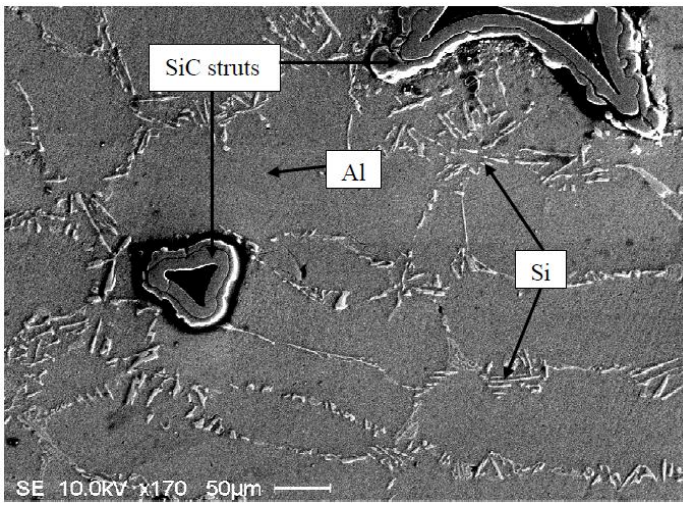

Figure 5. Microstructure of the A356/SiC foam composite subsequent to etching.

3.2 Friction coefficient

The steady state sliding friction coefficient characteristics for the A356 aluminum alloy matrix and A356/SiC foam composite against an alumina ball for different applied loads is shown in Figure 6 and also presented in Table 1, with their respective standard deviations. In general for

both materials the friction coefficients increase as the applied load is increased due to the process of wear. However, the matrix alloy increases at a faster rate than the composite material. An improvement of friction results from adding a cellular SiC reinforcement. It is thought that this may be due to carbon being released from the interior of the SiC struts and acting as a lubricant. This trend is in accord with the friction coefficient results obtained from Riahi et al. [7] for their Al/SiC/graphite hybrid composite. For example, at applied indentation loads of 5 N, 10 N and 20 N, the percent reduction in friction coefficients from the aluminum alloy to the composite are 16%, 31% and 34%, respectively. For both materials, the fact that the sliding distance and velocity are kept constant, suggests the friction coefficient is dependent on the applied load.

Table 1. Tribological friction and wear behavior of A356 alloy and A356/SiC foam composite materials at three different loads.

Load (N)	Friction coefficient, μ		Wear rate (m^3/m)*10^{-12}	
	A356	A356/SiC foam	A356	A356/SiC foam
5	0.37 ±0.01	0.31 ± 0.02	5 ±1.3	4 ±0.6
10	0.48 ±0.01	0.33 ±0.01	12 ±0.8	9 ±0.7
20	0.59 ± 0.01	0.39 ±0.02	28 ±0.3	25 ±0.4

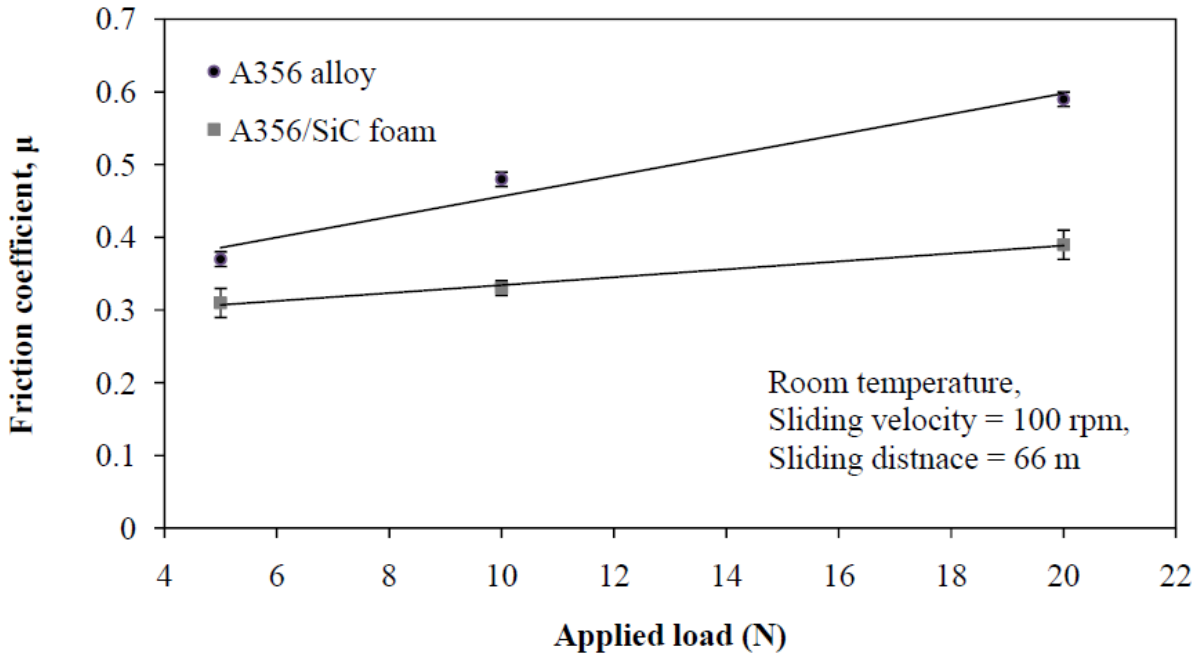

Figure 6. Friction coefficient versus load for the A356 aluminum alloy and the A356/SiC foam composite for three loads.

The typical behaviour of dry sliding coefficient of friction as a function of sliding distance for the three applied loads is depicted in Figure 7. At applied indentation loads of 5 N, 10 N and 20 N the friction coefficient for the A356 alloy initially increases slightly at the start of the test and gradually increases to steady state level and remains constant after a sliding distance of 8 m. In all three loading conditions the A356/SiC foam composite samples have a rapid increase in their friction coefficients reaching maximum values of approximately 0.48 to 0.51 at the start of the test followed by a gradual decrease to a constant steady state level after reaching sliding distances of 40 m, 35 m and 30 m, respectively. At greater distances or until the end of the test, the friction coefficient values of both materials do not have a substantial fluctuation which implies the steady state sliding friction coefficient is reached. As the applied load increases, a shorter sliding distance is required for the friction coefficient to reach a constant, stable value. After a running in period, the friction coefficient of the A356 aluminum alloy reaches a quicker, less variable, steady state than the A356/SiC foam composite.

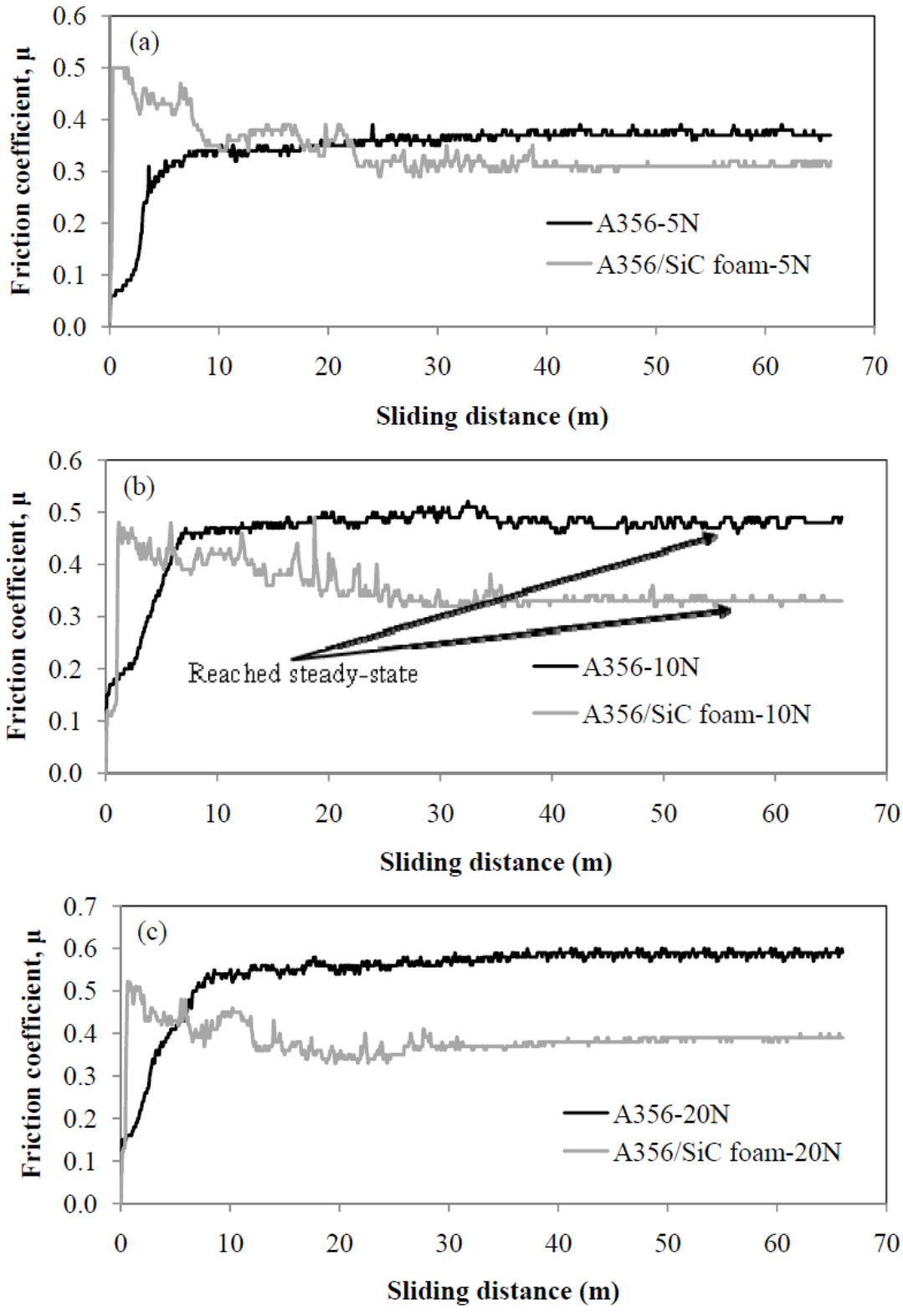

Figure 7. Friction coefficient versus sliding distance for A356 and A356/SiC foam composites. (a) 5 N, (b) 10 N, (c) 20 N.

As the A356 aluminum alloy plastically deforms during the wear process, a phenomenon of work hardening results creating a hardened sliding surface. A recent study conducted on wear properties of aluminum-silicon alloys established an increase of hardness in the wear track area as compared to the unworn areas [8]. The effects of the applied indentation loads of 0 N, 5 N, 10 N and 20 N on the hardness of the wear track areas were investigated. Vickers macrohardness measurements were performed on the as-cast A356 alloy and A356/SiC foam composite prior to and subsequent to the application of the normal loads. The Vickers macrohardness as a function of applied indentation load for both the unreinforced A356 aluminum alloy and A356/SiC foam are given in Figure 8 and presented in Table 2, with their respective standard deviations The results indicate with an increase in applied indentation load, the Vickers hardness of the wear track surface area increases in a linear relationship for both materials, indicative of work hardening. For example, the unreinforced A356 alloy and A356/SiC foam composite have an initial hardness of 84 ±2 kgf mm^{-2} and 69 ±2 kgf mm^{-2}, respectively. Under an applied normal load of 20 N, the unreinforced A356 alloy and A356/SiC foam composite have an increased hardness of 108 ±2 kgf mm^{-2} and 91 ±4 kgf mm^{-2}, respectively. Although monolithic SiC by-itself is typically harder than aluminum alloys, the bulk hardness of the composite is lower than the A356 alloy at all applied indentation loads. The SiC ceramic struts behave in a brittle manner when the indentation load is applied. The difference in this behavior may be sourced to the composite porosity, foam strut material and nature of the foam strut manufacturing process.

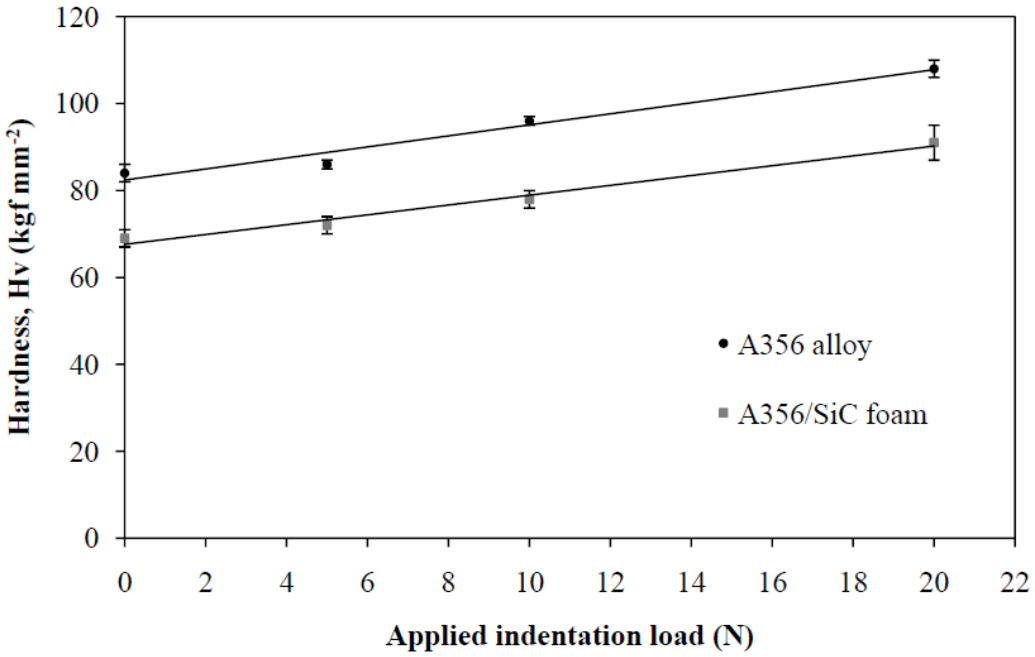

Figure 8. Vickers macrohardness as a function of applied indentation load.

Table 2. Vickers macrohardness of A356 alloy and A356/SiC foam composite.

	Applied loads (N)			
	0 N	5 N	10 N	20 N
Material	Hardness, Hv (5 kg)			
A356 alloy	84 ±2	86 ±1	96 ±1	108 ±2
A356/SiC foam	69 ±2	72 ±2	78 ±2	91 ±4

To evaluate the wear surface work hardening effect on the friction coefficient, the friction coefficient as a function of hardness for both the unreinforced A356 aluminum alloy and A356/SiC foam are given in Figure 9 with their respective standard deviations. The results demonstrate that hardness as well as the wear couple materials influences the friction between two mating materials. The friction coefficient of the alumina/A356 alloy couple of this study, increases linearly with surface hardness, greater for the unreinforced A356 alloy. For the same applied indentation load, the A356/SiC foam composite has a lower friction coefficient than the A356 alloy. As the sliding distance increases, the carbon at the interior of the composite foam

struts has a protective lubricating film effect on the overall composite by gradually releasing solid carbon lubricating material onto the wear surface, thus reducing the shear stresses. This resulted in a decrease in friction of the A356/SiC foam composite when compared to the A356 aluminum alloy. However, as the applied load is increased from 5 N to 20 N, the friction coefficient of the A356 alloy and A356/SiC foam composite increased by 59% and 26%, respectively. This phenomenon is consistent with a previous study of metals in sliding contact with alumina ceramic. The work consisted of alumina sliding on metals of copper, nickel and iron. The tests were performed in both a vacuum and in an oxygen atmosphere. The metals expose to oxygen experienced a higher friction coefficient then those exposed to vacuum. This was due to the strong interfacial bonds between the oxidized metal and alumina ceramic oxide [9]. Consequently, the ability of a metal to oxidize will influence the adhesive force during the dry sliding of a metal and alumina ceramic. Increased loading caused additional ploughing and surface contact between the alumina ball and A356 aluminum matrix, thus an increase in friction. To further investigate the behavior of hardness on friction coefficient, future work can include the sliding behavior of the A356 alloy and A356/SiC composite against a hard steel ball.

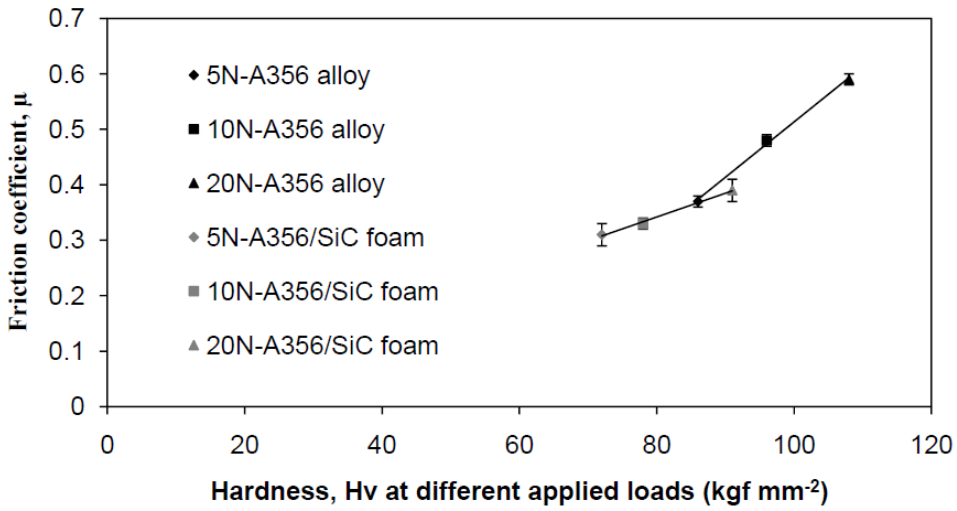

Figure 9. Friction coefficient as a function of hardness at different indentation loads.

3.3 Wear properties

The experimental wear rates as a function of applied load for the unreinforced A356 aluminum alloy and A356/SiC foam composite against an alumina ball for a fixed sliding distance of 66 m are given in Figure 10 and tabulated in Table 1 with their respective standard deviations. For both materials and the same constant rotational speed of 100 rpm, the wear rate increases as the applied load increases. Both materials show an approximate linear increase in wear rate as the load increases which indicates the applied load has a strong influence on the wear property. This behavior is in agreement with Wang et al. [10] for their (C+SiC)/Al composite based on a wood template. The wear rate is higher for the A356 aluminum alloy as compared to the A356/SiC foam composite for all loading conditions. With the incorporation of a 12 vol.% SiC network structure the results indicate a positive improvement on the wear resistance of the monolithic A356 alloy. The hardness of the SiC and softness of the carbon both help reduce the wear rate of the composite. For example, at applied indentation loads of 5 N, 10 N and 20 N the percent reduction in the wear rate from the aluminum alloy to the composite material are 20%, 25% and 10%, respectively.

Generally, in tribology dry wear tests, the concept of seizure arises when there is a lack of lubrication between two materials/surfaces in motion. Seizure of a specimen during a pin on disk test occurs when excess material is transferred from the disk to the pin causing a sticking or welding of mating parts. Prior to seizure, it is common to detect unusual noise and vibrations emanating from the assembly followed by a sudden stop in sliding between the mating parts. For the test conditions of this work, no seizure of the materials was observed. In a recent work, it was shown by adding 7% silicon to pure aluminum an improvement in seizure properties of pure aluminum was obtained [11]. Other studies have shown that Al-Si-Graphite composites exhibit

better seizure resistance than the base metal [12]. The enhancement arises from the formation of a graphite film on the mating surfaces. In addition, SiC particles dispersed in an aluminum alloy matrix displayed better seizure resistance than the matrix alloy [13]. Interestingly, the materials of the present study; A356 aluminum alloy and A356/SiC foam composite incorporate these features. The aluminum alloy contains 7.1% silicon in the aluminum matrix and the reinforcement is composed of carbon and SiC all of which reduce the tendency to seize.

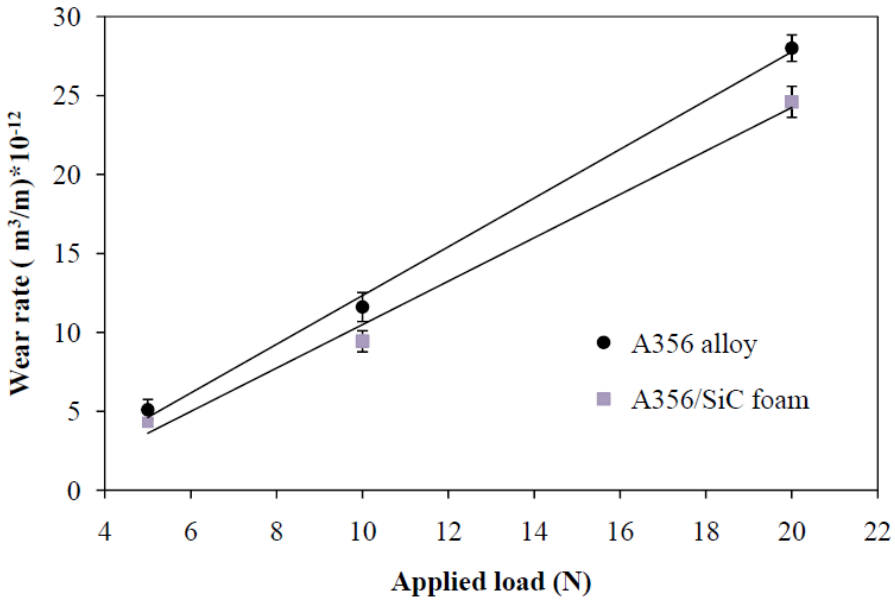

Figure 10. Wear rate versus load for the A356 aluminum alloy and the A356/SiC foam composite for three applied loads.

A typical comparison of the A356 alloy and A356/SiC foam composite cross-sections of the wear track width profiles for a 10 N applied load obtained from an optical surface profilometer are given in Figure 11. The results indicate that the un-reinforced A356 aluminum alloy has a larger wear profile than the composite. By incorporating a SiC network structure, the depth of wear penetration is reduced by approximately 20 μm at a 10 N load. On the inside and outside circumference of both wear track profiles there is material uplift due to the alumina ball penetrating inside the material causing plastic deformation as a result of the normal load applied.

On the outside edge, there is approximately 21 µm of material uplift for the A356 alloy, considerably more than the 4 µm for the A356/SiC foam composite.

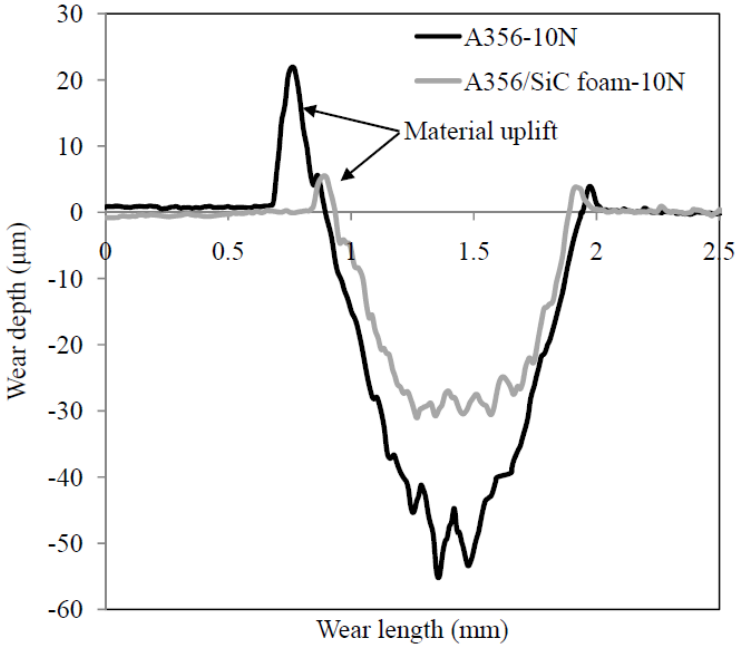

Figure 11. Typical wear track width profiles for 10 N normal load.

3.4 Examination of worn surfaces

Figure 12 shows the typical wear track (e.g. scar) patterns developed on the surfaces of the A356 aluminum profile alloy matrix (Figure 12 a, c, e) and A356/SiC foam composite (Figure 12 b, d, f) from the alumina ball at three different loads. To obtain detailed images from the wear tracks, SEM micrographs were taken at close proximity to the specimens. The edges of the samples are further away from the wear tracks. The width of the wear tracks were measured at four locations and averaged. By incorporating the SiC network reinforcement, at 5 N the A356 wear scar width decreased from 906 ±103 µm to 703 ± 81 µm, at 10 N the wear scar width decreased from 1125 ± 98 µm to 984 ±27 µm and at 20 N the wear scar width decreased from 1765 ±120 µm to 1593 ± 69 µm. This indicates the ceramic network structure is providing support to the aluminum

matrix. In addition, as the load increases both the A356 aluminum alloy and A356/SiC foam composites wear scar width increased due to ploughing of the alumina ball into the test materials.

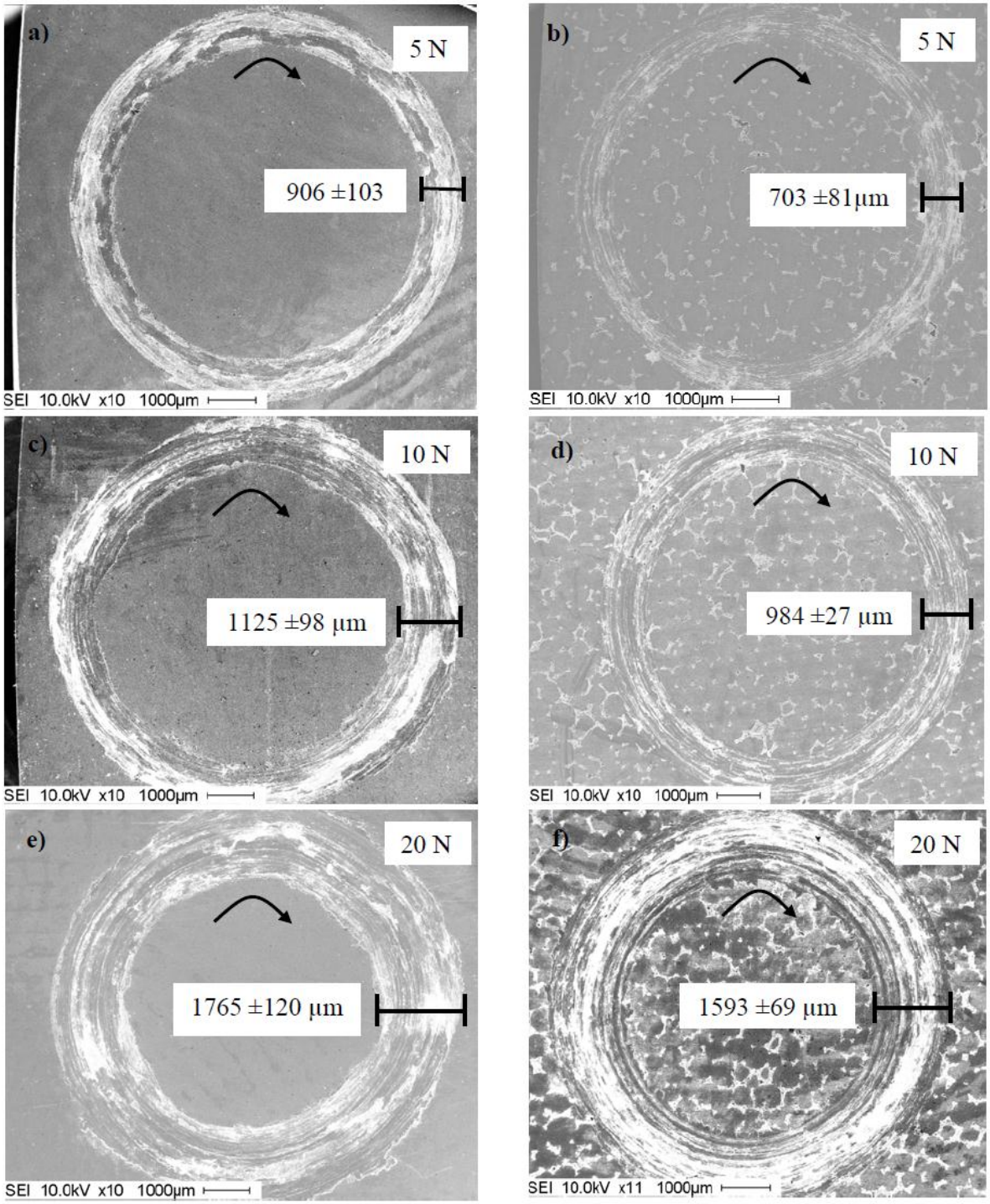

Figure 12. SEM wear surfaces of the A356 aluminum alloy ((a), (c), (e)) and the A356/SiC foam ((b), (d), (f)) composite for loads of 5 N, 10 N and 20 N. Arrow show the direction of motion of the specimens.

Typical worn surfaces of the unreinforced A356 aluminum alloy and A356/SiC foam composites were examined with SEM to understand the wear mechanisms. In both materials the wear track morphologies are not smooth, but characterized by continuous wear grooves and debris particles. During sliding, a rough surface signifies abrasive wear as some material is pulled out from the surface and forms loose abrasive particles while a smooth, smeared surface indicates adhesive wear from plastic deformation without any material removed from the surface. Figure 13 illustrates the typical A356 aluminum alloy after exposure to a 5 N load at 100 RPM for 30 minutes. Along the wear track, both wear mechanisms, abrasive and adhesive wear, are visible. At higher magnification, the abrasive wear is shown as a rough surface dispersed with small particles of debris.

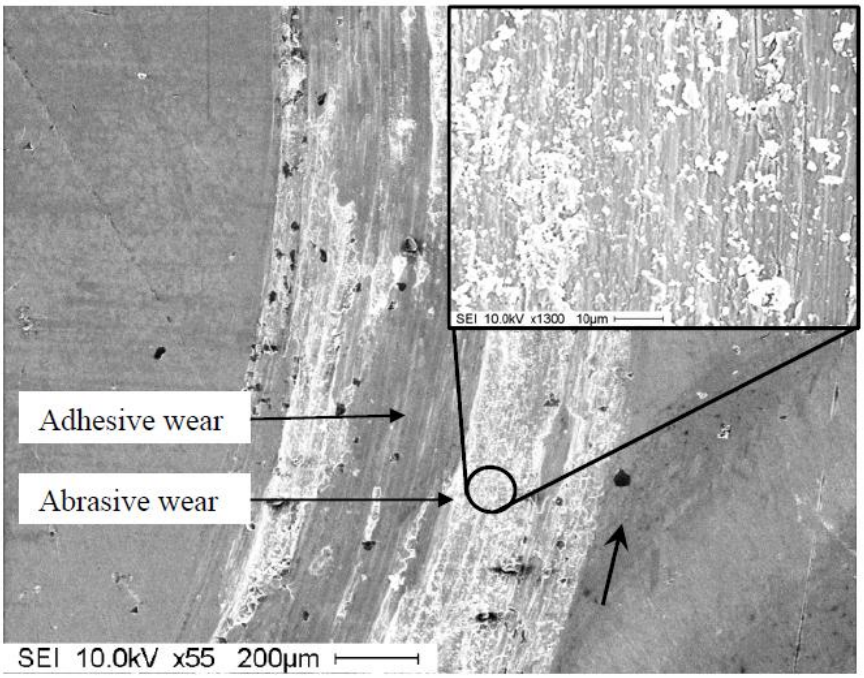

Figure 13. SEM of the A356-5N wear surface, arrow indicates the direction of rotation.

The worn surface of the pin, in this case a stationary, unlubricated, alumina ball was examined under SEM to understand the mode of wear. Initially adhesive wear develops between the two mating surfaces due to friction. Adhesive wear promotes transfer of material between the

two surfaces in contact. For example, the aluminum alloy adheres to the alumina ball as shown in Figure 14. As the sliding process proceeds, aluminum builds-up and eventually forms areas of metal to metal contact. Over time the material attached to the alumina ball has been dislodged and flakes off in the form of small wear debris particles. In other areas the softer aluminum tends to adhere in small patches to the outside of the bottom of the alumina ball. The alumina ball was examined with SEM and showed no signs of wear or material loss/spalling.

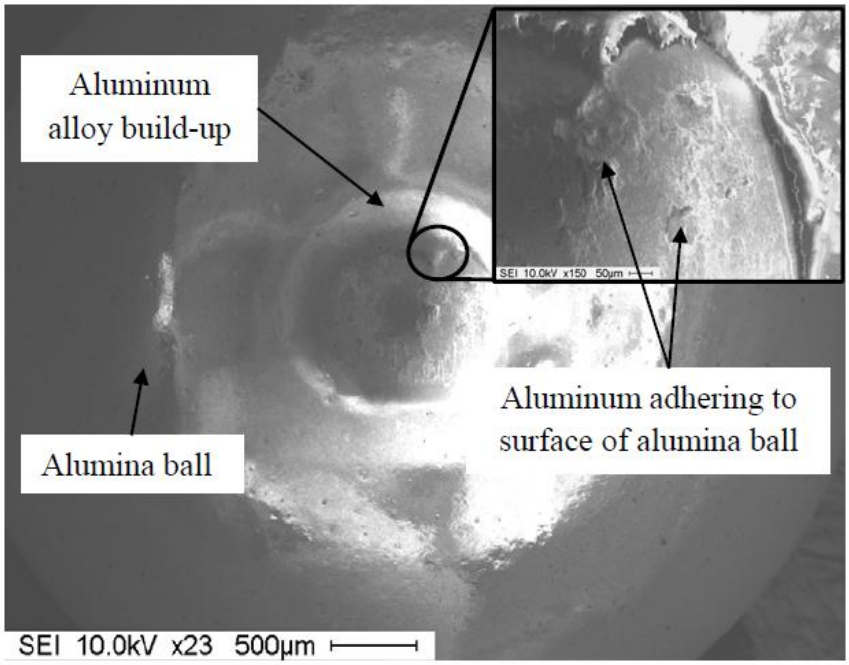

Figure 14. SEM of the counterpart alumina ball after dry sliding-A356-5N.

Figure 15 illustrates the typical A356/SiC foam composite after exposure to a 5 N load at 100 RPM for 30 minutes. Similar to the A356 alloy, the A356/SiC foam composites exhibits both abrasive and adhesive wear along the wear track sliding direction. The toughness of the alumina is greater than the SiC and carbon materials, thus both tend to fracture into small pieces under the applied load of the alumina ball. Studies on aluminum matrix composites incorporating ceramic particles have observed similar phenomenon: the debris particles can come loose, others may be embedded into the soft matrix while others may be crushed under the applied load

forming a film between the two contacting surfaces [14]. In this work, SiC and carbon particles are shown to have beneficial effects on the tribological properties of this composite. The SiC and carbon are shown to fracture into smaller pieces which produce wear debris particles. Other SiC particulates may prevent the penetration of the alumina sphere into the composite and thereby protect the softer aluminum from deforming and increases its wear resistance. SiC and carbon particles may get crushed into powders to produce a dual effect, wear resistance and friction coefficient reduction, respectively as observed in the wear rate and friction coefficient results.

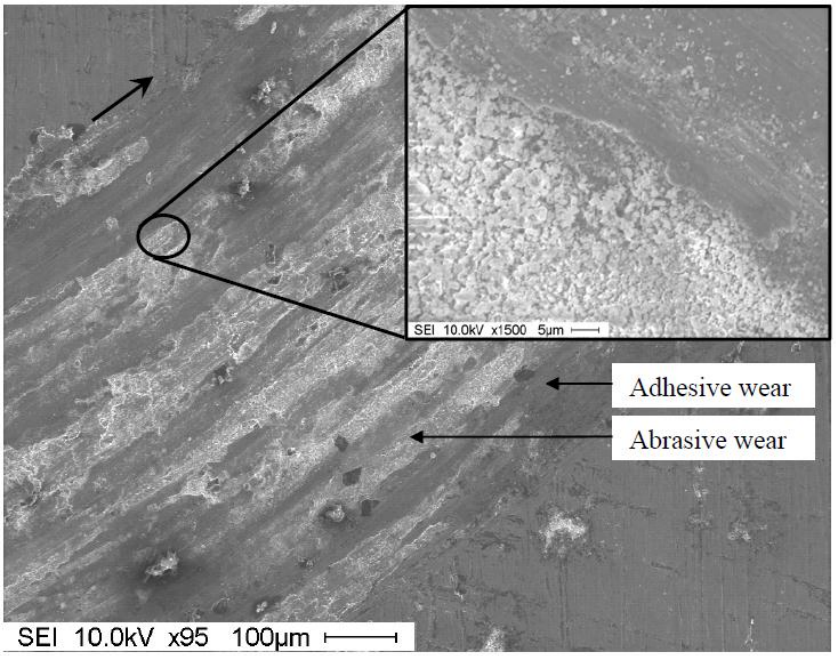

Figure 15. SEM of the A356/SiC-5N wear surface, arrow indicates the direction of rotation.

The magnified area of a typical wear track for the A356 alloy after subjecting it to a 20 N load at 100 RPM for 30 minutes is shown in Figure 16. As a result of the larger normal load, the soft aluminum has a greater amount of material uplift on the inner and outer circumferences of the wear track, as well as wider grooves, as compared to the 5 N loaded specimen. Both adhesive and abrasion wear are present. At a lower load, abrasion is the major wear mechanism while at higher loads adhesive is the main wear mechanism.The A356/SiC aluminum alloy after exposure

to a 20 N load at 100 RPM for 30 minutes shows the wear surface given in Figure 17. The micrograph shows mixed regions of adhesive and abrasive wear in addition to some material uplift on the circumference of the wear track. The magnified view of the wear track shows the cross-section outline of a triangular strut. Under the normal load of 20 N, both the brittle SiC ceramic and carbon interior tend to crush from the tougher alumina ball. However the decrease in wear and friction coefficient from that of the monolithic material, suggest the SiC and carbon are taking part in the wear mechanism. The groove size decreases in width indicating less plastic deformation when the SiC network is

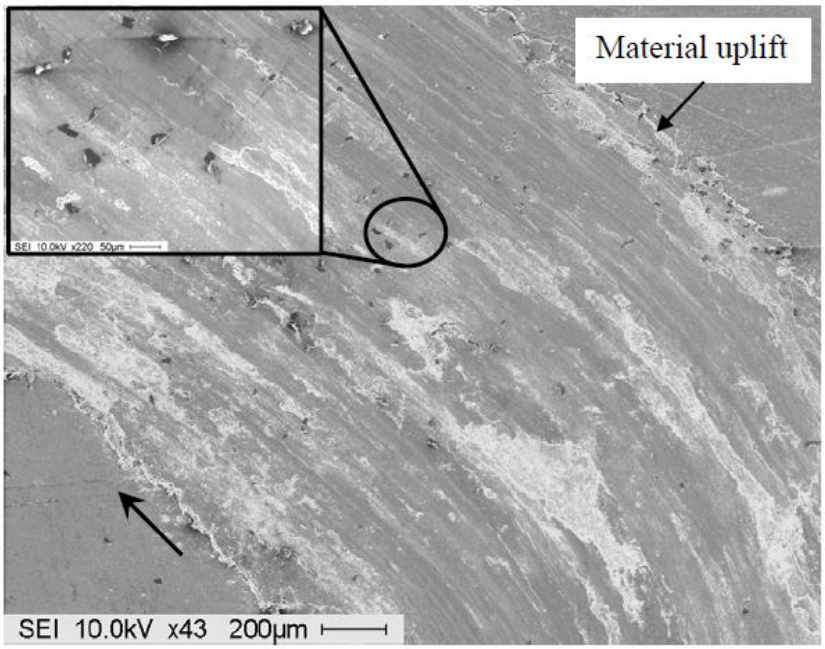

Figure 16. SEM of the A356-20N wear surface, arrow indicates the direction of rotation.

incorporated into the A356 alloy. Upon closer inspection of the SiC/C triangular strut in the wear path of the alumina ball given in Figure 18, the wear grooves in the aluminum alloy appear to stop at the boundary of the abraded strut. The immediate area surrounding the strut is smooth indicating less material removal by the alumina ball in this location. There is some smearing from the constituents of the strut material as depicted behind the strut. These observations may

be the reason why the composite demonstrates improved wear and friction coefficient properties as compared to the matrix alloy.

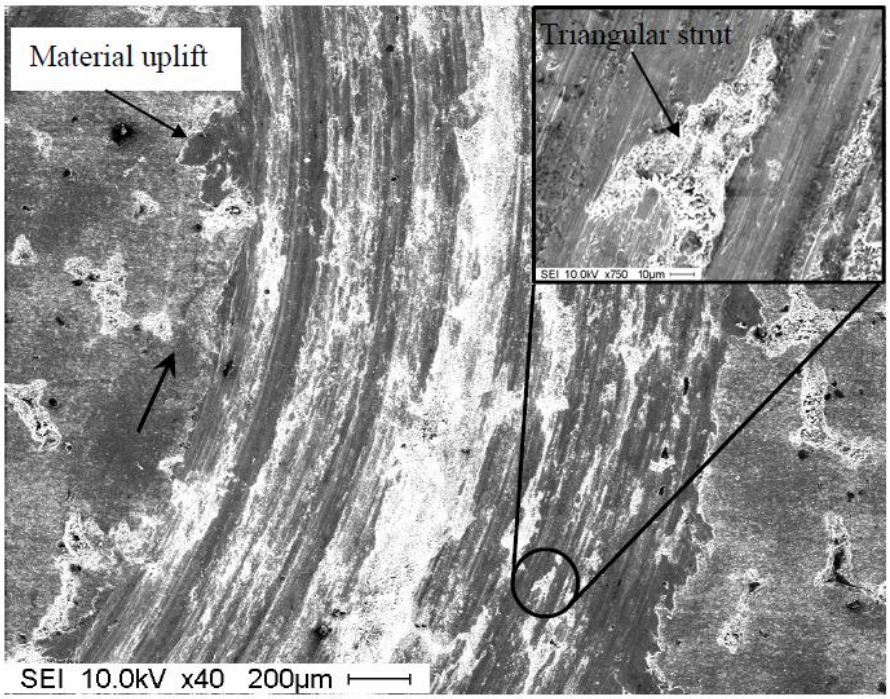

Figure 17. SEM of the A356/SiC-20 N wear surface, arrow indicates the direction of rotation.

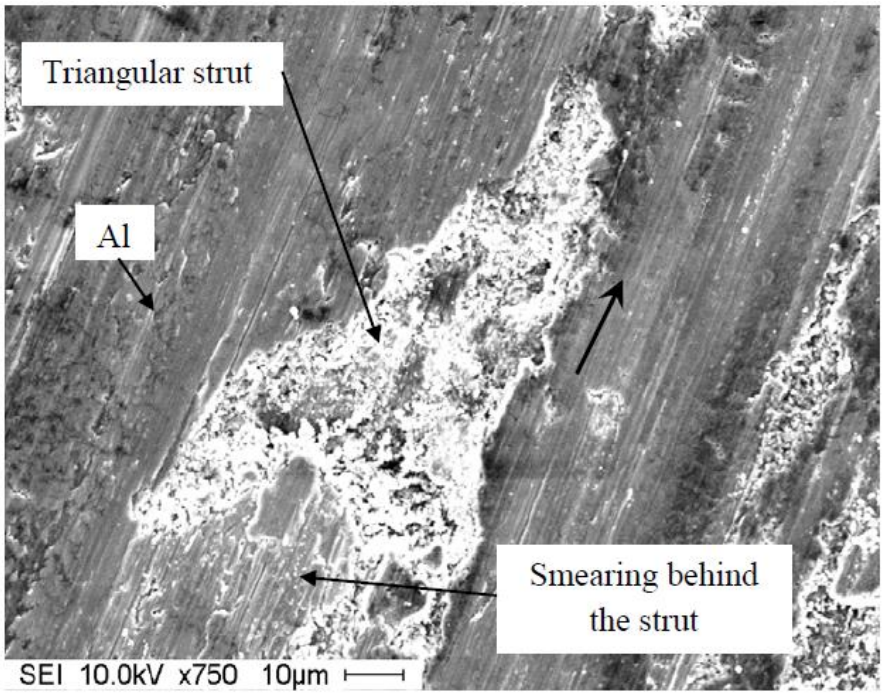

Figure 18. Magnified view of the wear track A356/SiC at 20 N showing the cross-section outline of the triangular abraded strut. Arrow indicates the direction of rotation.

3.5 Literature data comparison

The wear and friction behavior of aluminum/silicon carbide (Al/SiC) composites have been extensively investigated [15]. In particular, SiC particulates employed to reinforce a variety of aluminum alloys show a trend of increasing wear resistance and decreasing friction coefficient in contrast to the unreinforced aluminum alloys. However, trends in friction coefficients for Al/SiC materials are reported to be inconsistent with other investigations using similar Al/SiC materials. For instance, in one report, SiC particles improved the wear resistance but also increased the friction coefficient over the unreinforced aluminum alloy [16]. Due to a lack of development for a common testing procedure, the wear and friction coefficient results can differ and thus are numerically difficult to compare from study to study. While rarely mentioned in the literature, each wear and friction experimental result from different studies are unique to themselves because of the conditions the two opposing materials were exposed to; pin-on-disk, ball-on-disk and block-on-ring. In addition, examples of varying conditions from laboratory to laboratory can be a problem; the atmospheric humidity, wear procedure employed (normal load, specimen geometry, sliding speed, sliding distance, test duration) in addition to counter-face material and surface condition may have a dramatic effect on the results [17]. Comparing the numerical results from this work with that of others would be advantageous, however it would not be accurate since the experiments would have to be performed under the exact conditions [18]. For example, two separate studies have been conducted on a 2014 wrought aluminum alloy. In one study, Hosking et al. [19] carried out a pin-on-disk test on Al 2024/SiC_p (particle size 14µm, 20 wt%, sliding velocity 0.10 ms^{-1}, sliding distance 1000 m) and an SAE 52100 steel ball. Under an applied load of 0.5-4 N, the friction coefficient ranged from 0.23 to 0.35 for the 2024 aluminum alloy and 0.1 to 0.35 for the Al 2024/SiC_p composite. A composite wear rate of 0.95 $m^3/m \times 10^{-12}$

occurred after a sliding distance of 1000 m and applied load of 1000 g (9.81 N). Conversely, results of another work reported a pin-on-disk test on Al 2024/SiC_p (particle size 15μm, 20 wt%, sliding velocity 0.16 ms^{-1}, sliding distance 25 m) and an SAE 52100 steel ball showed under a load of 9.35 N, the friction coefficient was 0.6 ±0.2 and wear rate after 1000 m of 1.25 m^3/m x 10^{-12} for the Al 2024/SiC_p composite [20].

5.0 Conclusions

The dry sliding wear, friction coefficient and Vickers macrohardness for A356 and A356/SiC foam composite produced from a low-vacuum infiltration of A356 aluminum alloy into a porous SiC foam network structure was evaluated with a ball-on-disk apparatus. The wear rate and friction coefficient were reduced by the incorporation of the SiC network structure containing a carbon interior. However, the friction coefficient increased with hardness of the wear track due to the pin material employed. The composite has better tribological properties than the conventional aluminum alloy. The results obtained for this aluminum/silicon carbide interpenetrating phase composite wear and friction resistance study, signify the potential use of this novel engineering material in areas requiring wear resistance coupled with light-weight applications. The following conclusions can be drawn from the results of this study:

1. With the presence of only 12 vol% SiC, the wear rate and friction coefficient were improved for the imposed wear conditions of this study.
2. The friction coefficient decreased due to the lubricating effect of the carbon in the SiC struts as compared to the A356 aluminum alloy.
3. The improved wear rate of the composite is related to the hardness of the SiC and lubricating effect of the carbon.
4. The A356/SiC foam composite may be used as a self-lubricating composite.

5. A solid SiC foam strut composite may reduce the wear rate and wear track worn volume at higher loads due to a stronger supporting reinforcement structure.

Acknowledgements
The authors would like to thank the Natural Sciences and Engineering Research Council of Canada (NSERC) for the financial support.

References

[1] S. Suresha, B.K. Sridhara, Wear characteristics of hybrid aluminium matrix composites reinforced with graphite and silicon carbide particulates, Compos. Sci. Technol. 70 (2010) 1652-1659.

[2] D. Cree, M. Pugh, Production and characterization of a three-dimensional cellular metal-filled ceramic composite, J. Mater. Process. Tech. 210 (2010) 1905-1917.

[3] R. Raj, L.R. Thompson, Design of the microstructural scale for optimum toughening in metallic composites, Acta Metall. Mater. 42 (1994) 4135-4142.

[4] A. Daoud, M.T. AbouEl-khair, Wear and friction behavior of sand cast brake rotor made of A359-20 vol% SiC particle composites sliding against automobile friction material, Tribol. Int. 43 (2010) 544–553.

[5] H. Chang, J. Binner, R. Higginson, Dry sliding wear behaviour of Al(Mg)/Al_2O_3 interpenetrating composites produced by a pressureless infiltration technique, Wear 268 (2010) 166-171.

[6] F. Akhlaghi, A. Zare-Bidaki, Influence of graphite content on the dry sliding and oil impregnated sliding wear behavior of Al 2024-graphite composites produced by in situ powder metallurgy method, Wear 266 (2009) 37-45.

[7] A.R. Riahi, A.T. Alpas, The role of tribo-layers on the sliding wear behavior of graphitic aluminum matrix composites, Wear 251 (2001) 1396-1407.

[8] M. Kathiresan, T. Sornakumar, Friction and wear studies of die cast aluminum alloy-aluminum oxide-reinforced composites, Ind. Lubr. Tribol. 62 (2010) 361-371.

[9] S.V. Pepper, Effect of adsorbed films on friction of Al_2O_3,-metal systems, J. Appl. Phy. 47 (1976) 2579-2583.

[10] T.C. Wang, T.X. Fan, D. Zhang, G.D. Zhang, The fabrication and wear properties of C/Al and (C+SiC)/Al composites based on wood template, Mater. Lett. 60 (2006) 2695-2699.

[11] A.S. Reddy, B.N. Pramila Bai, K.S.S. Murthy, S.K. Biswas, Wear and seizure of binary Al-Si alloys, Wear 171 (1994) 115-127.

[12] S. Das, S.V. Prasad, T.R. Ramachandran, Tribology of A1-Si alloy-graphite composites: triboinduced graphite films and the role of silicon morphology, Mater. Sci. Eng. A138 (1991) 123-132.

[13] B.K. Prasad, K. Venkateswarlu, A.K. Jha, O.P. Modi, S. Das, R. Dasgupta, A.H. Yegneswaran, Sliding wear response of an Al-Cu alloy: the influence of SiC particle reinforcement and test parameters, J. Mater. Sci. Lett. 17 (1998) 1121-1123.

[14] A.M. Hassan, A.T. Mayyas, A. Alrashdan, M.T. Hayajneh, Wear behavior of Al-Cu and Al-Cu/SiC components produced by powder metallurgy, J. Mater. Sci. 43 (2008) 5368-5375.

[15] R. L. Deuis, C. Subramanian, J. M. Yellupb, Dry sliding wear of aluminum composites-a review, Compos. Sci. Technol. 57 (1997) 415-435.

[16] B. Venkataraman, G. Sundararajan, The sliding behaviour of Al/SiC particulate composites-I. Macrobehaviour, Acta. Mater. 44 (1996) 451-460.

[17] Standard test method for wear testing with a pin-on-disk apparatus, ASTM G99-05, American Society for Testing and Materials, West Conshohocken, PA.

[18] A.P. Sannino, H.J. Rack, Dry sliding wear of discontinuously reinforced aluminum composites: review and discussion, Wear 189 (1995) 1-19.

[19] F.M. Hosking, F.F. Portillo, R. Wunderlin, R. Mehrabian, Composites of aluminium alloys: fabrication and wear behaviour, J. Mater. Sci. 17 (1982) 477-498.

[20] A.T. Alpas, J.D. Embury, Sliding and abrasive wear behavior of an aluminum (2014)-SiC particle reinforced composite Scripta. metall. mater. 24 (1990) 931-935.